

***k* ordering of atomic energy levels and its relation to the spectroscopic quantum defects**

R. M. Sternheimer

Brookhaven National Laboratory, Upton, New York 11973

(Received 29 January 1979)

The *k*-ordering properties of the spectra of atoms and ions consisting of a single valence electron outside a core of closed shells ( $k = n + l$ ) have been introduced and discussed extensively in four previous papers, together with the constant *l* sequences within each group of levels having the same value of *k* (*k* bands). In the present paper, it is demonstrated that the spectroscopic quantum defects  $\delta_{nl}$  play the role of the "order parameter" for the *k*-ordering phase of the excited-state spectra. Thus only penetrating orbitals, i.e., those having a large  $\delta_{nl}$  ( $\delta_{nl} \gtrsim 0.2$ ), exhibit the phenomenon of *k* ordering, and in particular, the curves of  $\delta_{nl}$  vs *l* (for fixed *k*) are generally curved downwards, with an abrupt decrease to values of  $\delta_{nl}$  close to zero at the limiting angular momentum  $l_1$ , which has been previously introduced. The curves of  $\delta_{nl}$  vs *l* are basically similar to the curves of magnetic field  $\tilde{H}$  as a function of temperature *T* in a ferromagnet, with an abrupt decrease to  $\delta_{nl} \sim 0$  at  $l_1$ , which can therefore be regarded as the analog of the Curie temperature  $T_C$ . The "reduced quantum defects"  $\eta_{nl} \equiv \delta_{nl} + l - l_1$  (for  $l \leq l_1$ ) have also been introduced. It is shown that the ordering of the  $\eta_{nl}$  values for  $l \leq l_1$  determines the nature of the *l* patterns of the spectrum, e.g., *dpsf*, *dpfs*, or *pdsf*.

## I. INTRODUCTION

In four previous papers,<sup>1-4</sup> I have introduced the concept of the quantum number

$$k = n + l \quad (1)$$

as an energy-ordering quantum number for the excited-state energy levels of the neutral alkali-metal atoms (i.e., Na, K, Rb, and Cs) and the singly ionized alkaline-earth atoms (i.e., Mg<sup>+</sup>, Ca<sup>+</sup>, Sr<sup>+</sup>, Ba<sup>+</sup>, and Ra<sup>+</sup>),<sup>1</sup> and, in addition, states with one electron outside closed shells in the spectra of groups IB, IIA, IIB, and IIIA elements of the Periodic Table, and their isoelectronic ions.<sup>2</sup> For the spectra of Ref. 1, we have considered a total<sup>1,3</sup> of 416 excited states, while for the spectra of Ref. 2, we have analyzed a total<sup>2,3</sup> of 858 additional energy levels, giving a combined total of 1274 levels, which provide overwhelming evidence for the existence of a phenomenon which we have called "*k* ordering," namely, the grouping together of levels having the same value of *k* and having nearly the same energy (term value in the spectrum). Thus, the excited states of each spectrum can be divided into successive *k* groups, and within each *k* group (or "*k* band"), the levels increase (slightly) in energy according to a fixed sequence of *l* values, which we have called the "*l* pattern." Except in a few cases, the *l* pattern does not change with increasing *k*, and, as an outstanding example, the *l* pattern is *pdsf* for a total of 158 excited states of rubidium from  $k = 6$  to  $k = 55$ , i.e., over a range of fifty *k* values.

The *k* ordering and the *l* sequences of the levels have been exhibited specifically in nine *j*-averaged spectra in Ref. 1 and in ten *j*-averaged spectra in

Ref. 2. By *j*-averaged spectra, we mean that we have averaged the energy values  $E_{n,l,j}$  listed in the tables of Moore<sup>5</sup> using the weighting factors  $(2j + 1)$  for the two levels with  $j = l + \frac{1}{2}$  and  $j = l - \frac{1}{2}$ , so as to average over the effects of the fine structure. Altogether, a total of 42 spectra have been analyzed in this fashion, and the *l* patterns of these spectra have been tabulated in Table XIV of Ref. 2. In addition, Ref. 3 contains the revised and corrected spectra of Ga I and Sr I (which had been previously discussed in Ref. 2); these corrected spectra were obtained in part from the more recent papers of Johansson and Litzén<sup>6</sup> (Ga I) and of Garton and Codling<sup>7</sup> (Sr I).

Two important concepts introduced in Refs. 2 and 3 are those of the limiting ionicity  $\delta_1$  (where  $\delta \equiv Z - N$  and *N* is the number of electrons in the atom or ion considered) and the limiting angular momentum  $l_1$ . Thus it has been shown in Ref. 2 (see pp. 469-471) that if the ionicity  $\delta$  exceeds  $\delta_1$ , there is a phase transition from *k* ordering to hydrogenic ordering (denoted by "H ordering"), i.e., energy ordering according to the principal quantum number *n*. The approximate phase diagram of  $\delta_1$  as a function of the atomic number *Z* is shown in Fig. 2 of Ref. 2.

In a similar manner, as discussed in Ref. 3, there exists also a limiting angular momentum  $l_1$  for *k* ordering, such that if *l* is made larger than  $l_1$ , a phase transition from *k* ordering to hydrogenic ordering (according to *n*) will occur, for those atoms and ions which lie within the region of ionicities  $\delta \leq \delta_1$ . The phase diagram of *l* vs *Z*, i.e., the approximate curve of  $l_1$  vs *Z* which separates the two phases, is given in Fig. 1 of Ref. 3. A qualitative explanation of the absence of *k* order-

ing for  $l > l_1$  in terms of the overlap of the valence and the core wave functions has been given by the author in Ref. 3 (see p. 1755). A somewhat different explanation, which also discusses some general features of the  $k$  ordering, has been given in a recent paper of Foley.<sup>8</sup> In Ref. 8, Foley has discussed the  $k$  ordering from the point of view of the spectroscopic quantum defects and the phase shifts for elastic scattering at zero energy, utilizing a relation previously discovered by Seaton.<sup>9</sup>

In the present paper, we will also discuss the relation of the  $k$  ordering to the quantum defects  $\delta_{nl}$ . It may be noted that most of the work of the present paper, including Figs. 1-5, Tables I and II, and the definition of  $\eta_{nl}$ , was completed before we were informed about Foley's paper.

In Sec. II, we will show that the spectroscopic quantum defects  $\delta_{nl}$  play the role of the "order parameter" for the  $k$  ordering. Thus, as discussed in Ref. 3, only penetrating orbitals, i.e., those having a large  $\delta_{nl}$  ( $\delta_{nl} \geq 0.2$ ) exhibit the phenomenon of  $k$  ordering, and moreover the curves of  $\delta_{nl}$  vs  $l$  (for fixed  $k$ ) are generally concave downwards, and basically similar to the curves of magnetic field  $\bar{H}$  as a function of temperature  $T$  in a ferromagnet, with an abrupt decrease to zero at the limiting angular momentum  $l_1$ , which therefore can be regarded as the analog of the Curie temperature  $T_C$ . Of course, instead of the magnetic field analogy, we could have used the behavior of any classical order parameter below the transition point for the appropriate phase transition.

In Sec. III, we will define a quantity which we have called the "reduced quantum defect," denoted by  $\eta_{nl}$ , for each level  $nl$ . The reduced quantum defects  $\eta_{nl}$  are directly related to the energy ordering of the  $nl$  levels *within each  $k$  group* (or " $k$  band"), i.e., they are related to the  $l$  pattern of the spectrum, as discussed above and in Refs. 1-4. Finally, in Sec. IV, we give a brief summary and discussion of the results of the present paper.

## II. RELATION OF THE $k$ ORDERING TO THE SPECTROSCOPIC QUANTUM DEFECTS $\delta_{nl}$

We have calculated the spectroscopic quantum defects  $\delta_{nl}$  for the large majority of the levels included in the 19 spectra of Refs. 1, 2, and 4. The quantum defects  $\delta_{nl}$  are obtained from the following modified Rydberg formula for the one-electron energy levels:

$$L - E_{nl} = (1 + \delta)^2 \mathcal{R}_\infty / (n - \delta_{nl})^2, \quad (2)$$

where  $\delta \equiv Z - N$  is the ionicity,  $\mathcal{R}_\infty$  = Rydberg unit =  $109\,737 \text{ cm}^{-1}$ ,  $L$  is the series limit, and  $E_{nl}$  is the energy of the level  $nl$  as measured from the

TABLE I. Spectrum of the neutral rubidium atom Rb I. The excitation energies  $E_{nl}$  (in units of  $\text{cm}^{-1}$ ) are measured from the ground state (5s). The corresponding spectroscopic quantum defects  $\delta_{nl}$  as obtained from Eq. (3) are listed in the last column of the table. The series limit  $L$  is  $33\,691.1 \text{ cm}^{-1}$ . The values of  $E_{nl}$  are the  $j$ -averaged excitation energies, as derived from the tables of Moore (see Table IV of Ref. 1).

$nl$	$k$	$E_{nl} (\text{cm}^{-1})$	$\delta_{nl}$
5s	5	0	3.195
5p	6	12 737	2.712
4d	6	19 355	1.233
6s	6	20 134	3.155
6p	7	23 767	2.675
5d	7	25 702	1.294
7s	7	26 311	3.144
4f	7	26 792	0.012
7p	8	27 858	2.663
6d	8	28 689	1.316
8s	8	29 047	3.139
5f	8	29 278	0.013
5g	9	29 298	$\approx 0$
8p	9	29 848	2.656
7d	9	30 281	1.327
9s	9	30 499	3.137
6f	9	30 628	0.014
6g	10	30 637	$\approx 0$
9p	10	30 966	2.654
8d	10	31 222	1.333
10s	10	31 362	3.136
7f	10	31 442	0.015
6h	11	30 644	$\approx 0$
10p	11	31 659	2.651
9d	11	31 832	1.317
11s	11	31 917	3.135
8f	11	31 969	0.017
11p	12	32 117	2.650
10d	12	32 228	1.339
12s	12	32 295	3.134
12p	13	32 436	2.649
11d	13	32 515	1.340
13p	14	32 667	2.648
12d	14	32 725	1.342
31p	32	33 554.5	2.657
30d	32	33 557.0	1.394
32s	32	33 559.2	3.156
29f	32	33 559.9	0.079
32p	33	33 563.6	2.663
31d	33	33 566.0	1.383
33s	33	33 567.7	3.179
30f	33	33 568.5	0.082
49p	50	33 639.9	2.704
48d	50	33 640.5	1.431
50s	50	33 641.0	3.199
47f	50	33 641.3	$\approx 0.08$
Limit		33 691.1	

TABLE II. Spectrum of the singly ionized lead ion  $Pb^+$  ( $Pb II$ ). The excitation energies  $E_{nl}$  (in units of  $cm^{-1}$ ) are measured from the  $6p_{1/2}$  ground state. The corresponding spectroscopic quantum defects  $\delta_{nl}$  as obtained from Eq. (3) (with  $\delta=+1$ ) are listed in the last column of the table. The series limit  $L$  is  $121\,243\,cm^{-1}$ . The values of  $E_{nl}$  are the  $j$ -averaged excitation energies, as derived from the tables of Moore (see Table VII of Ref. 2).

$nl$	$k$	$E_{nl} (cm^{-1})$	$\delta_{nl}$	$nl$	$k$	$E_{nl} (cm^{-1})$	$\delta_{nl}$
6p	7	9387	4.019	11d	13	114491	2.937
7s	7	59448	4.335	12p	13	114685	3.819
6d	8	69274	3.094	13s	13	115496	4.261
7p	8	76334	3.874	10f	13	115655	1.137
8s	8	89180	4.300	9g	13	115797	0.022
5f	8	92520	1.091	12d	14	115901	2.935
7d	9	94896	2.918	13p	14	116037	3.818
8p	9	95851	3.842	14s	14	116615	4.261
9s	9	101346	4.303	11f	14	116729	1.139
6f	9	102874	1.112	10g	14	116833	0.023
5g	9	103559	0.018	13d	15	116912	2.933
8d	10	103872	2.973	14p	15	117008	3.819
9p	10	104821	3.830	12f	15	117521	1.140
10s	10	107930	4.258	11g	15	117600	0.023
7f	10	108533	1.123	14d	16	117660	2.932
6g	10	108968	0.020	13f	16	118121	1.143
9d	11	109304	2.937	12g	16	118183	0.023
10p	11	109734	3.824	15d	17	118230	2.930
11s	11	111574	4.262	14f	17	118588	1.142
8f	11	111942	1.130	13g	17	118637	0.022
7g	11	112230	0.021	16d	18	118675	2.926
10d	12	112444	2.937	14g	18	118996	0.023
11p	12	112726	3.806	17d	19	119027	2.926
12s	12	113912	4.262	15g	19	119286	0.023
9f	12	114147	1.135	Limit		121243	
8g	12	114346	0.022				

ground state, taken as zero, i.e., the values listed in Refs. 1, 2, and 4, as obtained by  $j$ -averaging over the values given in the tables of Moore.<sup>5</sup> The difference  $n - \delta_{nl}$  is often referred to as the effective quantum number  $n_{nl}^*$ .

Upon solving Eq. (2) for  $\delta_{nl}$ , we obtain

$$\delta_{nl} = n - (1 + \delta) \left( \frac{\mathcal{R}_\infty}{L - E_{nl}} \right)^{1/2} = n - n_{nl}^* . \quad (3)$$

As examples of the calculated values of  $\delta_{nl}$ , we have listed these values in Tables I and II for the spectra of Rb I and Pb II, respectively. The  $j$ -averaged values of  $E_{nl}$  were obtained from Table IV of Ref. 1, and Table VII of Ref. 2, respectively. Of course, in the usual spectroscopic notation Rb I refers to the spectrum of the neutral rubidium atom, and Pb II refers to the spectrum of the  $Pb^+$  ion. It can be seen from these results that except for low-lying states,  $\delta_{nl}$  is approximately independent of  $n$  for a given  $l$ , and that  $\delta_{nl}$  decreases rapidly and monotonically to a value close to zero as  $l$  is increased to  $l = l_1$ , where  $l_1 = 3$  for Rb and

$l_1 = 4$  for  $Pb^+$ .

Thus we were led to graph  $\delta_{nl}$  as a function of  $l$  for a number of atomic and ionic spectra. For definiteness, we have plotted  $\delta_{nl}$  vs  $l$  for constant  $k$ , even though the variation of  $\delta_{nl}$  with  $n$  and therefore with  $k$ , at a given  $l$ , is generally small, as discussed above. We present three examples of these graphs in Figs. 1-3, which show  $\delta_{nl}$  vs  $l$  for Sn II ( $Sn^+$  spectrum) for  $k=8$ , and for Cs I and Pb II for  $k=9$ . If we define  $l_1$  as the lowest value of  $l$  for which  $\delta_{nl} \approx 0$ , we find  $l_1 = 3$  for Sn II and Cs I, and  $l_1 = 4$  for Pb II.

We note that a very approximate representation of  $\delta_{nl}$  is given by the straight line

$$\delta_{nl} \sim l_1 - l , \quad (4)$$

and we have shown this 45° line in Figs. 1-3, with  $l_1 = 3$  for Sn II and Cs I, and  $l_1 = 4$  for Pb II. If the relation  $\delta_{nl} = l_1 - l$  would be exact, we would have a degeneracy of the levels within each  $k$  band, which has been called " $k$  degeneracy" in the paper of Foley,<sup>8</sup> in which a very similar equation has

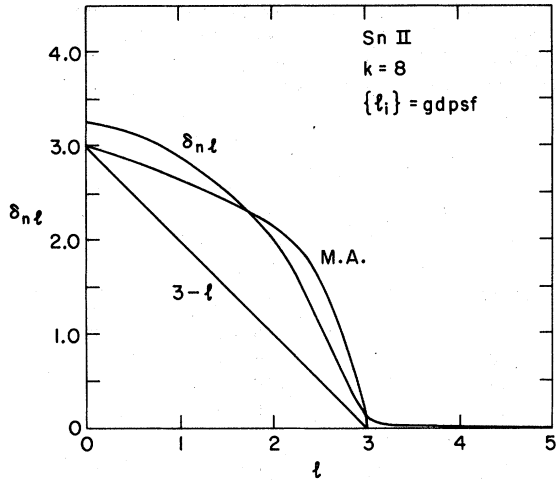


FIG. 1. Spectroscopic quantum defect  $\delta_{nl}$  for the  $\text{Sn}^{II}$  spectrum ( $\text{Sn}^+$  ion) as a function of  $l$ , for fixed  $k=8$ . We note the abrupt decrease of  $\delta_{nl}$  as  $l$  approaches the limiting angular momentum  $l_1=3$ . For  $l > l_1$ , the  $\delta_{nl}$  are very small ( $\delta_{nl} \lesssim 0.1$ ). The curve marked "M.A." refers to the magnetic analogy discussed in the text [Sec. II, discussion following Eq. (5)]. The qualitative agreement of  $\delta_{nl}$  with the M. A. curve strengthens the validity of regarding  $\delta_{nl}$  as the appropriate "order parameter" for  $k$  ordering. The straight line  $3-l=l_1-l$  refers to the approximation of  $\delta_{nl}$  by Eq. (4).

been considered, namely,  $\delta_l = g - l$  [Eq. (2) of Ref. 8]. This degeneracy can be easily derived from Eqs. (2) and (4), since we would then obtain

$$L - E_{nl} \cong \frac{(1+\delta)^2 \mathcal{R}_\infty}{(n+l-l_1)^2} = \frac{(1+\delta)^2 \mathcal{R}_\infty}{(k-l_1)^2}. \quad (5)$$

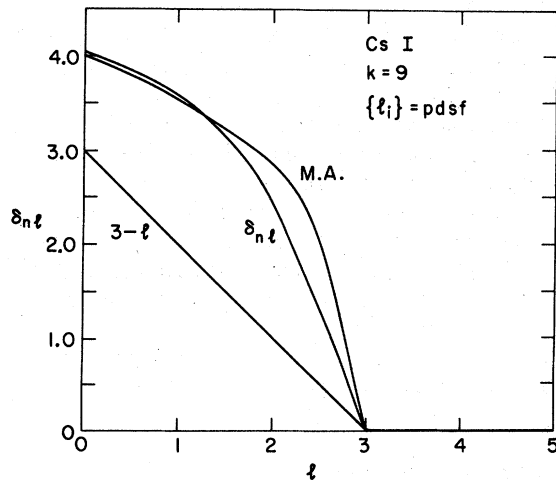


FIG. 2. Spectroscopic quantum defect  $\delta_{nl}$  for the Cs spectrum (CsI) as a function of  $l$ , for fixed  $k=9$ . The limiting angular momentum  $l_1$  is 3. The curve M. A. (magnetic analogy) approximates the behavior of  $\delta_{nl}$  very closely. The approximation  $l_1-l=3-l$  is shown for comparison.

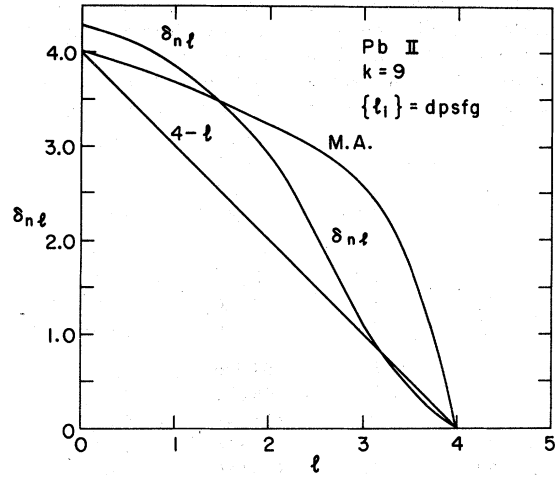


FIG. 3. Spectroscopic quantum defect  $\delta_{nl}$  for the  $\text{Pb}^+$  spectrum ( $\text{Pb}^{II}$ ) as a function of  $l$ , for fixed  $k=9$ . The curve M. A. (magnetic analogy) and the straight line  $l_1-l=4-l$  are shown for comparison.

Equation (4) would imply that  $\delta_{nl}$  decreases by one unit as  $l$  is increased by one unit, and Foley<sup>8</sup> has derived this approximate relationship using Seaton's relation<sup>9</sup> for the elastic scattering phase shifts and the calculations of these phase shifts by Manson.<sup>10</sup>

From the preceding discussion and from Eqs. (4) and (5), it is clear that the deviations of  $\delta_{nl}$  from the value  $l_1-l$  are directly responsible for the spread of the energy levels within a given  $k$  band, and for the resulting  $l$  pattern of the spectrum. This situation has led us to define the "reduced quantum defects"  $\eta_{nl}$ , which will be discussed in Sec. III.

We wish now to discuss the property of  $\delta_{nl}$  as the appropriate order parameter for the  $k$  ordering. As we have anticipated in the Introduction, (Sec. I), the curves of  $\delta_{nl}$  vs  $l$  are similar to the curve of  $\bar{H}$  vs  $T$  (magnetic field versus temperature) in a ferromagnet, below the Curie temperature  $T_C$ . For this reason, we have plotted a curve having the same shape as the curve of spontaneous magnetic moment versus  $T$  for angular momentum  $J \rightarrow \infty$  in Figs. 1-3. These curves are denoted by MA ("magnetic analogy"). The maximum of the MA curve was taken as  $l_1$  or  $l_1+1$  and the corresponding value of  $T_C$  was taken as  $l_1$ . The shape of the curve, which involves the Brillouin function  $B_J$ , was obtained from the textbook of Eyring *et al.*<sup>11</sup>

It is seen that the MA curves approximate  $\delta_{nl}$  much more closely than the linear approximation of Eq. (4), in particular for  $\text{Sn}^{II}$  (Fig. 1) and  $\text{Cs}^I$  (Fig. 2). Thus the results of Figs. 1-3 give additional support to the concept of a  $k$  ordering phase,

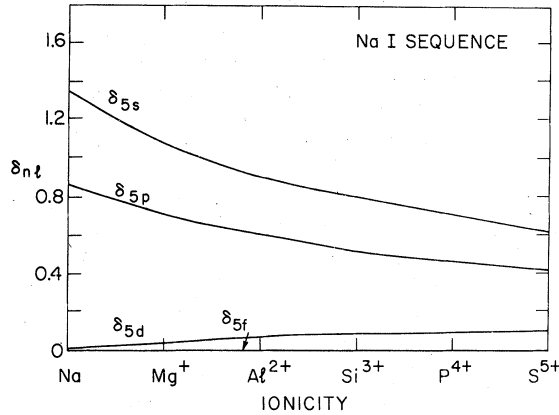


FIG. 4. Spectroscopic quantum defects  $\delta_{5s}$ ,  $\delta_{5p}$ ,  $\delta_{5d}$ , and  $\delta_{5f}$  ( $\approx 0$ ) for the Na I isoelectronic sequence, as a function of the ionicity. We note the smooth behavior of the  $\delta_{nl}$  as the ionicity  $\delta$  traverses the phase boundary between  $k$  ordering (for  $\text{Mg}^+$ ) and hydrogenic ordering (for  $\text{Al}^{2+}$ ).

which was introduced by the author in Ref. 2, and furthermore they establish the validity of considering  $\delta_{nl}$  as the relevant order parameter for the  $k$  phase, with the angular momentum  $l$  taking place of the temperature  $T$  in the analogous thermodynamical system (and  $l_1$  analogous to  $T_c$ ).

Since  $\delta_{nl}$  vanishes approximately for  $l > l_1$ , i.e., at the transition from  $k$  ordering to H ordering, it occurred to us that perhaps when the ionicity  $\delta$  is made too large, i.e., as  $\delta$  becomes larger than the limiting ionicity  $\delta_1$ , the quantum defects  $\delta_{nl}$  may also undergo a similar discontinuity or abrupt change. For this reason, we have plotted in Figs. 4 and 5 the typical quantum defects  $\delta_{5s}$ ,  $\delta_{5p}$ ,  $\delta_{5d}$ , and  $\delta_{5f}$  for the Na I and Rb I isoelectronic sequences, respectively, as a function of the ionicity  $\delta$ . The neutral atom and its isoelectronic ions are listed on the abscissa axis of the two figures. It is immediately apparent that no such discontinuity occurs at the limiting ionicity, which is  $\delta_1 \sim 1.5$  for the Na I sequence and  $\delta_1 \sim 2$  for the Rb I sequence (see Fig. 2 of Ref. 2). In particular, for the Na I sequence, where an abrupt phase transition occurs between  $\text{Mg}^+$  ( $k$  ordering) and  $\text{Al}^{2+}$  (H ordering) (see Fig. 1 of Ref. 2), the quantum defects  $\delta_{nl}$  are completely smooth in this region of ionicity  $\delta$ .

A possible explanation of the smooth behavior in Figs. 4 and 5 as contrasted to the abrupt decrease of  $\delta_{nl}$  in Figs. 1–3 may well be the fact that when  $l$  is made too large, i.e., for  $l > l_1$ , the overlap of the valence wave function  $v_0(nl)$  with the core wave functions  $u_0(n_c l_c)$  and their perturbations  $u_1(n_c l_c \rightarrow l'_c)$  which leads to the  $k$  ordering<sup>3,4</sup> becomes vanishingly small, whereas no such rapid

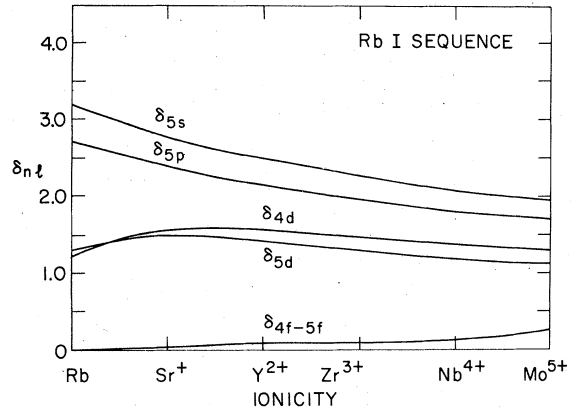


FIG. 5. Spectroscopic quantum defects  $\delta_{5s}$ ,  $\delta_{5p}$ ,  $\delta_{4d}$ ,  $\delta_{5d}$ , and  $\delta_{4f-5f}$  for the Rb I isoelectronic sequence, as a function of the ionicity. We note the smooth behavior of the  $\delta_{nl}$  as the ionicity  $\delta$  traverses the phase boundary between  $k$  ordering and hydrogenic ordering at  $\delta_1 \sim 2$  (corresponding to the  $\text{Y}^{2+}$  ion).

change of the overlap occurs as the ionicity is increased beyond  $\delta_1$ .

### III. REDUCED QUANTUM DEFECTS $\eta_{nl}$

As discussed in Sec. II, it is useful to define the “reduced quantum defects”  $\eta_{nl}$  as follows:

$$\eta_{nl} \equiv \delta_{nl} - (l_1 - l) = \delta_{nl} + l - l_1 \quad (l \leq l_1), \quad (6)$$

$$\eta_{nl} \equiv \delta_{nl} \quad (l \geq l_1), \quad (7)$$

where we have used two different definitions for the regions  $l \leq l_1$  and  $l \geq l_1$ . Of course, for  $l \geq l_1$ ,  $\delta_{nl}$  is always small (generally  $\delta_{nl} < 0.1$ ), and the definition of Eq. (7) ensures that  $\eta_{nl}$  is always positive for  $l \geq l_1$ , since  $\delta_{nl} > 0$  in all cases.

From Eq. (6), we can derive the relation

$$\delta_{nl} = \eta_{nl} - l + l_1 \quad (l \leq l_1) \quad (8)$$

so that the denominator  $(n - \delta_{nl})^2$  of Eq. (2) can be written

$$\begin{aligned} (n - \delta_{nl})^2 &= (n + l - l_1 - \eta_{nl})^2 \\ &= (k - l_1 - \eta_{nl})^2 \quad (l \leq l_1). \end{aligned} \quad (9)$$

For  $l > l_1$ , hydrogenic ordering prevails and the energy levels are practically degenerate with the level  $n = n_1$ , where  $n_1$  is defined by

$$n_1 \equiv k - l_1. \quad (10)$$

Thus we can write, both for  $l \leq l_1$  and for  $l \geq l_1$ , the following general equation for the binding energy  $L - E_{nl}$  of all levels with a given value of  $k$ :

$$L - E_{nl} = \frac{(1 + \delta)^2 \mathcal{R}_\infty}{(k - l_1 - \eta_{nl})^2} = \frac{(1 + \delta)^2 \mathcal{R}_\infty}{(n_1 - \eta_{nl})^2}. \quad (11)$$

As an example, for the case of RbI, the  $k$  band with  $k=50$  contains besides the levels  $49p$ ,  $48d$ ,  $50s$ , and  $47f$ , which are listed in Table IV of Ref. 1, also the following 43 levels which are essentially degenerate with  $47f$ , due to the hydrogenic ordering for  $l > l_1$  ( $l_1=3$ ):  $47g$ ,  $47h$ ,  $47i$ , ...,  $n=47, l=45$ , and  $n=47, l=46$ . Thus the  $k=50$  band contains a total of

$$k - l_1 = 50 - 3 = 47 \quad (12)$$

levels.

The approximate location of a given  $k$  band can be obtained from the Rydberg formula

$$L - E_k \simeq (1 + \delta)^2 \mathcal{R}_\infty / (k - l_1)^2. \quad (13)$$

Of course, for RbI, we have  $\delta = 0$  (zero ionicity). Thus Eq. (13) with  $k - l_1 = 47$  gives for the  $k=50$  band

$$L - E_{50} \simeq \mathcal{R}_\infty / 47^2 = 49.7 \text{ cm}^{-1}, \quad (14)$$

so that  $E_{50} \simeq 33\,691.1 - 49.7 = 33\,641.4 \text{ cm}^{-1}$ , which is near the upper limit of the  $k=50$  band at  $E_{47f} = 33\,641.3 \text{ cm}^{-1}$ .

The separation of levels with the same  $l$  in neighboring  $k$  bands can be obtained from the derivative  $\partial E_k / \partial k$ , which is obtained from Eq. (13), where  $L$ ,  $\delta$ , and  $l_1$  are constants:

$$\frac{\partial E_k}{\partial k} = \frac{2(1 + \delta)^2 \mathcal{R}_\infty}{(k - l_1)^3}. \quad (15)$$

Thus the spacing between the  $nl=46f$  and  $47f$  levels is given approximately by using the average  $k=49.5$ ,

$$\Delta E_k(49, 50) = 2\mathcal{R}_\infty / (49.5 - 3)^3 = 2.18 \text{ cm}^{-1}. \quad (16)$$

The order of magnitude of the average spacing  $\langle \Delta_{l_a l_b}(k) \rangle$  between successive  $l$  levels which obey  $k$  ordering ( $l_a, l_b \leq l_1$ ) in the  $k$ -band region can be obtained as follows. As we have discussed in Ref. 3 (see pp. 1757 and 1758), the separation  $S_{k, k+1}$  between the  $k$  and  $k+1$  bands is of the same order of magnitude as the spacing  $\Delta_{l_a l_b}(k)$  of levels within each  $k$  band (or may be even smaller for heavy atoms). If we assume that

$$S_{k, k+1} \sim \langle \Delta_{l_a l_b}(k) \rangle, \quad (17)$$

then between successive levels with  $l=l_1$ , i.e., between the levels  $nl_1$  and  $n+1, l_1$ , we have  $l_1+1$  intervals [e.g.,  $l_1=3$  intervals involving the levels  $49p$ ,  $48d$ ,  $50s$ ,  $47f$  in Table IV of Ref. 1, for Rb, plus one interval  $S_{49, 50}$  between  $46f$  ( $k=49$ ) and  $49p$  ( $k=50$ )], so that the average interval between successive  $k$  band levels is of the order of

$$\langle \Delta_{l_a l_b}(k) \rangle \simeq \frac{1}{(l_1 + 1)} \frac{\partial E_k}{\partial k} = \frac{2(1 + \delta)^2 \mathcal{R}_\infty}{(l_1 + 1)(k - l_1)^3}. \quad (18)$$

For Rb, with  $k=49.5$ ,  $l_1=3$ , Eqs. (16) and (18) give

$$\langle \Delta_{l_a l_b}(k) \rangle = \frac{2.18}{4} \text{ cm}^{-1} = 0.55 \text{ cm}^{-1}. \quad (19)$$

As we have discussed in Sec. II, the deviations of the  $\delta_{nl}$  from the values  $l_1 - l$ , i.e., the reduced quantum defects  $\eta_{nl}$  are directly responsible for the width of each  $k$  band and the  $l$  pattern ( $l$  sequence) of the levels  $nl$  within the  $k$  band. It is therefore of interest to plot the graphs of  $\eta_{nl}$  vs  $l$  (for constant  $k$ ) for several representative spectra. First we wish to note that if the  $l$  pattern is  $\{l_i\} = l_a l_b l_c l_d$ , i.e., if the levels  $n_a l_a, n_b l_b, n_c l_c, n_d l_d$  are arranged in the order of increasing energy, then according to Eq. (11), we must have the inequalities:

$$\eta_{n_a l_a} > \eta_{n_b l_b} > \eta_{n_c l_c} > \eta_{n_d l_d}. \quad (20)$$

Thus the level with the largest (algebraic) value of  $\eta_{nl}$  lies lowest, and the other levels with the same  $k$  value are arranged in the order of decreasing  $\eta_{nl}$  values.

In Figs. 6–8, we have plotted the values of  $\eta_{nl}$  vs  $l$  for nine representative spectra, namely, Ca I, Ga I, Sn II (Fig. 6); K I, Rb I, Ba II (Fig. 7); and Cs I, Tl I, Pb II (Fig. 8). The values of  $k$  and  $l_1$  as well as the  $l$  pattern are listed in the upper right-hand corner of the figures. The graphs of Fig. 6 pertain to  $k=8$ , whereas those of Figs. 7 and 8 pertain to  $k=9$ . Since the values of  $\delta_{nl}$  and

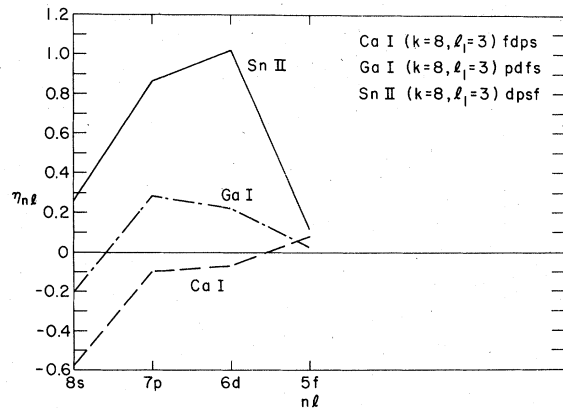


FIG. 6. Reduced quantum defects  $\eta_{nl}$ , as defined by Eq. (6), as a function of  $l$  for the  $k=8$  energy levels of the spectra Ca I, Ga I, and Sn II. The corresponding  $nl$  levels are listed on the abscissa. We note that the  $l$  pattern  $\{l_i\} = l_a l_b l_c l_d$  in each case corresponds to the sequence of decreasing  $\eta_{nl}$  values

$$\eta_{n_a l_a} > \eta_{n_b l_b} > \eta_{n_c l_c} > \eta_{n_d l_d}$$

[see Eq. (20)]. The values of  $k$  and  $l_1$ , and the  $\{l_i\}$  patterns are listed in the upper right-hand corner of the figure.

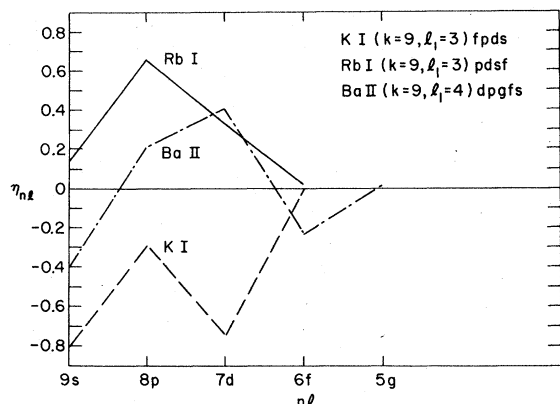


FIG. 7. Reduced quantum defects  $\eta_{nl}$ , as defined by Eq. (6), as a function of  $l$  for the  $k=9$  energy levels of the spectra KI, RbI, and BaII. The corresponding  $nl$  levels are listed on the abscissa.

hence those of  $\eta_{nl}$  are not sensitive to the value of  $n$ , as discussed above, they are also not sensitive to the difference between  $k=8$  and  $k=9$ . We may also note that  $l_1=3$  for the light and medium atoms ( $Z \leq 55$ ), whereas  $l_1=4$  for the heavy atoms ( $Z \geq 56$ ).

The most striking feature of these graphs is that with the exception of two spectra (namely, CaI in Fig. 6 and KI in Fig. 7), the two highest  $\eta_{nl}$  values involve the  $np$  and  $nd$  states, whereas the two lowest  $\eta_{nl}$  values involve the  $ns$  and  $nf$  levels. (Here we have not included the three  $\eta_{5g}$  values.) Thus we expect that four  $l$  patterns will be dominant, namely,  $dpsf$ ,  $pdsf$ ,  $dpfs$ , and  $pdfs$ . Indeed, if we consider the results of Table XIV of Ref. 2, we see that the most prevalent  $l$  patterns among the 42 spectra investigated are  $dpsf$ ,  $dpfs$ ,  $pdsf$ , and  $fdfs$ . Three of these  $l$  patterns are among those listed above. The fourth  $l$  pattern, mentioned

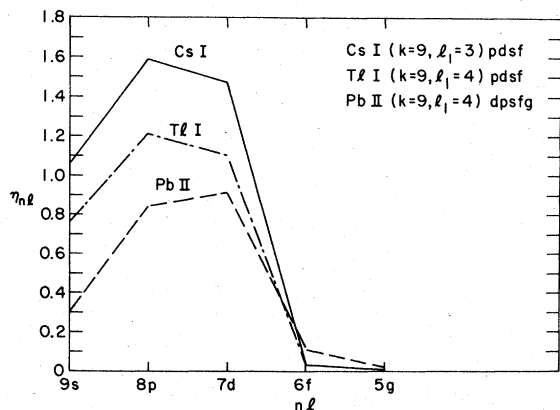


FIG. 8. Reduced quantum defects  $\eta_{nl}$ , as defined by Eq. (6), as a function of  $l$  for the  $k=9$  energy levels of the spectra CsI, TlI, and PbII. The corresponding  $nl$  levels are listed on the abscissa.

above, namely,  $pdfs$ , actually occurs in three cases, namely, CuI ( $k=5-8$ ), ZnI, and GaI (instead of the two cases listed in Table XIV of Ref. 2). The additional case, namely, GaI, is found to have the  $l$  pattern  $pdfs$ , when the revised spectrum of Johansson and Litzén<sup>6</sup> is used (see Table I of Ref. 4).

The two spectra which we have excluded above, namely, CaI in Fig. 6 and KI in Fig. 7, correspond to the patterns  $fdfs$  and  $fpds$ , respectively. The  $l$  pattern  $fdfs$  is found in ten spectra (see Ref. 2, Table XIV), exclusively among the light elements, with  $Z$  values ranging from  $Z_{\min}=11$  to  $Z_{\max}=33$ . The other  $l$  pattern, namely,  $fpds$ , is found only for the CaI spectrum (levels with  $k=5$  and  $k \geq 11$ ), besides the case of KI shown in Fig. 7.

The general tendency for the plots of  $\eta_{nl}$  vs  $l$  to have their highest values for  $np$  and  $nd$  states is obviously related to the predominant frequency of the  $l$  patterns  $dpsf$ ,  $dpfs$ , and  $pdsf$  which account for 32 cases out of a total of 48 which are listed in Ref. 2 (Table XIV). We believe that the maxima of  $\eta_{nl}$  at  $np$  and  $nd$  are due to the finer details of the valence-core overlap, which is believed to be responsible for the  $k$ -ordering phenomenon,<sup>3,4</sup> as well as the inverted fine structure of excited  $d$ ,  $f$ , and  $g$  levels.<sup>4</sup>

#### IV. SUMMARY AND DISCUSSION

In the present paper, we have investigated certain aspects of  $k$  ordering (and the associated  $l$  patterns) of atomic and ionic energy levels, which had not been discussed in our previous papers on this subject (Refs. 1-4). More specifically, we have investigated the relation of the  $k$  ordering of atomic energy levels  $E_{nl}$  to the corresponding spectroscopic quantum defects  $\delta_{nl}$ . The quantum defects  $\delta_{nl}$  had been briefly considered in Ref. 4 [see Eq. (2)], but their general relationship to the  $k$  ordering has only been discussed in the present paper, and independently in a recent paper of Foley.<sup>8</sup>

In connection with the discussion of Secs. II and III of the present paper, the author apologizes for the rather frequent cross references to the earlier papers of Refs. 1-4. However, in order to avoid needless duplication of the tables of Refs. 1-4 (altogether 35 tables) and of the four pertinent figures, it seemed desirable to write this paper as was done here, including the cross references. For those readers who are interested in the  $k$ -ordering properties of atomic and ionic spectra, and their associated  $l$  patterns, the four aforementioned papers should be studied in sequence.

In Sec. II of the present paper, we have discussed in detail the behavior of the quantum de-

fect  $\delta_{nl}$  as a function of the orbital angular momentum quantum number  $l$  (see Figs. 1–3). In particular, it has been shown for three representative cases (Sn II, Cs I, and Pb II) that the curves of  $\delta_{nl}$  vs  $l$  have a pronounced downward curvature and that  $\delta_{nl}$  decreases abruptly to a value close to zero at the limiting angular momentum  $l_1$  for  $k$  ordering, which has been introduced in Ref. 3. Here the value of  $l_1$  is 3 for Sn II and Cs I, and 4 for the Pb II spectrum. The curves of  $\delta_{nl}$  vs  $l$  (which have been obtained actually for the large majority of the 19 spectra considered in Refs. 1 and 2) show a remarkable similarity to the curves of magnetic field  $\bar{H}$  as a function of the temperature  $T$  in a ferromagnet, with an abrupt decrease to zero at the limiting angular momentum  $l_1$ , which therefore can be regarded as the analog of the Curie temperature  $T_C$ . The corresponding curves have been shown also in Figs. 1–3, where they have been labeled as “MA” for “magnetic analogy.” This similarity leads us to interpret the quantum defect  $\delta_{nl}$  as the classical order parameter for  $k$  ordering. In other words, the  $k$  ordering is a property of the penetrating orbitals with relatively low  $l$  values, such that  $l \leq l_1$ , for which the overlap of the valence electron wave function with the core orbitals is sufficiently large. It should also be mentioned that the existence of such a readily available order parameter as the quantum defect  $\delta_{nl}$  provides additional support for our previous assumption of a “ $k$ -ordering phase,” as was done in Refs. 2 and 3, and for the interpretation in terms of phase transitions at the limiting angular momentum  $l_1$  and the limiting ionicity  $\delta_1$ . We also note from Figs. 1–3, that since the curve of  $\delta_{nl}$  vs  $l$  does not have a discontinuity at  $l=l_1$ , but instead approaches the value  $\delta_{nl}(l_1)$  with a finite slope, the phase transition at  $l=l_1$  can be described technically as a second-order phase transition.

A less accurate approximation to the quantum defects  $\delta_{nl}$  is the straight line  $\delta_{nl} \sim l_1 - l$ , which has been introduced in Eq. (4) and is also shown in Figs. 1–3 for the spectra of Sn II, Cs I, and Pb II. A similar straight-line relationship, namely,  $\delta_{nl} \sim g - l$ , has also been considered by Foley.<sup>8</sup>

The approximate relation of Eq. (4) has led us to introduce the “reduced quantum defects”  $\eta_{nl}$ , which are defined by Eqs. (6) and (7) in Sec. III, in particular:  $\eta_{nl} \equiv \delta_{nl} + l - l_1$  for  $l \leq l_1$ . It is shown in Sec. III that the ordering of the  $\eta_{nl}$  values determines the  $l$  pattern within each group of levels having the same value of  $k$ , i.e., within the same  $k$  band. A general expression for the energy levels  $E_{nl}$  in terms of  $\eta_{nl}$  has been derived in Eqs. (8)–(11). From Eqs. (11) and (13), we have derived the expression for the separation of levels with

the same  $l$  in neighboring  $k$  bands, namely, the derivative  $\partial E_k / \partial k$  of Eq. (15). In addition, the average spacing  $\langle \Delta_{l_a l_b}(k) \rangle$  between successive  $l$  levels (with  $l \leq l_1$ ) in the  $k$  band is given by Eq. (18).

From Eq. (11), it is readily seen that the levels within a given  $k$  band are energy-ordered as follows:

$$E_{n_a l_a} < E_{n_b l_b} < E_{n_c l_c} < E_{n_d l_d},$$

if we have

$$\eta_{n_a l_a} > \eta_{n_b l_b} > \eta_{n_c l_c} > \eta_{n_d l_d}.$$

Thus the level with the highest algebraic  $\eta_{nl}$  value lies lowest, and the other levels with the same  $k$  value are arranged in the order of decreasing  $\eta_{nl}$  values, corresponding to the  $l$  pattern  $\{l_i\} = l_a l_b l_c l_d$ .

In Figs. 6–8, we have plotted the values of  $\eta_{nl}$  vs  $l$  for nine representative spectra, as explained in Sec. III. The most striking feature of these graphs is that with the exception of two spectra (Ca I and K I), the two highest  $\eta_{nl}$  values involve the  $np$  and  $nd$  levels, while the two lowest  $\eta_{nl}$  involve the  $ns$  and  $nf$  levels. Thus we expect that four  $l$  patterns will be dominant, namely,  $dpsf$ ,  $pdsf$ ,  $dpfs$ , and  $pdfs$ , and this expectation is generally borne out by the frequencies of the actual  $l$  patterns, as presented in Table XIV of Ref. 2.

After the work of the present paper was completed, we received a copy of a short paper of Ostrovsky,<sup>12</sup> in which the connection between  $k$  ordering and the spectroscopic quantum defects  $\delta_{nl}$  has also been considered. In particular, it was also pointed out that the relative constancy of the sum  $\delta_{nl} + l$  within a given  $k$  group is a necessary condition for the existence of  $k$  ordering, in similarity to Eq. (4) above, and to Eq. (2) of the paper of Foley.<sup>8</sup> In this connection, we can also refer to the paper of Demkov and Ostrovsky<sup>13</sup> and to the earlier papers of Klechkovskii<sup>14</sup> on the validity of the “ $n+l$  rule” for the ground states of neutral atoms.

Returning to the  $k$  ordering and the  $l$  patterns of the excited states of atoms and ions, as discussed in this series of five papers, there remains the wider question as to the fundamental significance of these remarkable regularities and their connection to the inverted fine structure (see Ref. 4) and to the large quadrupole antishielding factors<sup>15, 16</sup>  $\gamma_\infty$  and  $R$  for the atoms and ions having at least one filled  $np$  shell, and preferably a large number of filled  $np$  and  $nd$  shells (medium and heavy atoms with  $Z \geq 11$ ). As we have already discussed in Refs. 1 and 4, unless a  $p$  shell of the core is fully occupied, i.e., unless  $Z \geq 11$ , the  $k$  ordering does not occur and simultaneously the



excited  $d$  (and/or  $f$ ) states do not exhibit the inverted fine structure which is characteristic of the heavier elements. Also the ionic antishielding factor  $\gamma_\infty$  which depends directly on the large  $np \rightarrow p$  and  $nd \rightarrow d$  excitations of the core does not become large until  $Z \geq 11$ . In this connection, we note that the values of  $\gamma_\infty$  for monovalent ions with an external  $nd^{10}$  configuration, namely,  $\gamma_\infty(\text{Cu}^+) = -15.0$ ,<sup>17</sup>  $\gamma_\infty(\text{Ag}^+) = -34.9$ ,<sup>17</sup> and  $\gamma_\infty(\text{Au}^+) = -72.0$ ,<sup>18</sup> can be fitted by a formula similar to Eqs. (9), (10), and (12) of Ref. 4, namely,

$$\gamma_\infty[nd^{10}] = -0.9847(Z - 15)^{1.0320} \quad (29 \leq Z \leq 79). \quad (21)$$

In Ref. 3 (see pp. 1755 and 1756), we have discussed the possibility that the  $k$  ordering is strongly dependent on the overlap of the valence wave function  $v(nl)$  and the core wave functions  $u_0(n_c l_c)$  and their perturbations  $u_1(n_c l_c \rightarrow l'_c)$  caused by the electrostatic interaction with the valence electron.

This possibility is enhanced to the status of a strong probability by the discovery in the present paper that the quantum defects  $\delta_{nl}$  are the appropriate order parameters for the  $k$  ordering, which has been found to occur only when  $\delta_{nl}$  is large ( $\delta_{nl} \geq 0.2$ ), i.e., for the penetrating orbitals with  $l \leq l_1$ . A similar explanation involving the number of radial states of the core which are occupied for a given  $l$  value has been put forward by Foley.<sup>8</sup>

#### ACKNOWLEDGMENTS

I wish to thank Professor H. M. Foley for several helpful discussions and for sending me a copy of his paper in advance of publication. I am also indebted to Dr. V. J. Emery for valuable comments. The present work was supported by the U. S. Department of Energy under Contract No. EY-76-C02-0016.

<sup>1</sup>R. M. Sternheimer, Phys. Rev. A **15**, 1817 (1977).

<sup>2</sup>R. M. Sternheimer, Phys. Rev. A **16**, 459 (1977).

<sup>3</sup>R. M. Sternheimer, Phys. Rev. A **16**, 1752 (1977).

<sup>4</sup>R. M. Sternheimer, Phys. Rev. A **19**, 474 (1979).

<sup>5</sup>C. E. Moore, *Atomic Energy Levels*, U. S. Natl. Bur. Stand. Circ. No. 467 (U. S. GPO, Washington, D.C., 1949-1958), Vols. I-III.

<sup>6</sup>I. Johansson and U. Litzén, Ark. Fys. **34**, 573 (1967).

<sup>7</sup>W. R. S. Garton and K. Codling, J. Phys. B **1**, 106 (1968).

<sup>8</sup>H. M. Foley, Phys. Rev. A **19**, 2134 (1979).

<sup>9</sup>M. J. Seaton, Compt. Rend. **240**, 1317 (1955).

<sup>10</sup>S. T. Manson, Phys. Rev. **182**, 97 (1969).

<sup>11</sup>H. Eyring, D. Henderson, B. J. Stover, and E. M. Eyring, *Statistical Mechanics and Dynamics* (Wiley, New York, 1964), p. 295.

<sup>12</sup>V. N. Ostrovsky, abstract of contributed paper to the

Sixth International Conference on Atomic Physics, Riga, USSR, 1978 (unpublished), p. 517.

<sup>13</sup>Yu. N. Demkov and V. N. Ostrovsky, Zh. Eksp. Teor. Fiz. **62**, 152 (1972) [Sov. Phys. JETP **35**, 66 (1972)].

<sup>14</sup>V. M. Klechkovskii, Dokl. Akad. Nauk SSR **80**, 603 (1951); Zh. Eksp. Teor. Fiz. **23**, 115 (1952); and **41**, 465 (1962) [Sov. Phys. JETP **14**, 334 (1962)].

<sup>15</sup>R. M. Sternheimer, Phys. Rev. **80**, 102 (1950); **84**, 244 (1951); **95**, 736 (1954); **105**, 158 (1957); **146**, 140 (1966); **164**, 10 (1967); Phys. Rev. A **6**, 1702 (1972).

<sup>16</sup>H. M. Foley, R. M. Sternheimer, and D. Tycko, Phys. Rev. **93**, 734 (1954); R. M. Sternheimer and H. M. Foley, *ibid.* **102**, 731 (1956); R. M. Sternheimer, *ibid.*

**130**, 1423 (1963); **132**, 1637 (1963); **159**, 266 (1967).

<sup>17</sup>R. M. Sternheimer, Phys. Rev. **146**, 140 (1966), see Table VI.

<sup>18</sup>R. P. Gupta and S. K. Sen, Phys. Rev. A **8**, 1169 (1973).